Author Manuscript

Author Manuscript

Author Manuscript

Author Manuscript

HHS Public Access

Author manuscript

Proteomics. Author manuscript; available in PMC 2020 February 01.

Published in final edited form as:

Proteomics. 2019 February ; 19(3): e1800213. doi:10.1002/pmic.201800213.

In vitro and *in vivo* proteomic comparison of human neural progenitor cell-induced photoreceptor survival

Melissa K. Jones[1,2], **Bin Lu**[1,2], **Dawn Z. Chen**[3,4], **Weston R. Spivia**[3], **Augustus T. Mercado**[1,2], **Alexander V. Ljubimov**[1,2,4], **Clive N. Svendsen**[1,2], **Jennifer E. Van Eyk**[3,4], and **Shaomei Wang**[1,2,4]

[1]Department of Biomedical Sciences, Cedars-Sinai Medical Center

[2]Board of Governors Regenerative Medicine Institute, Cedars-Sinai Medical Center

[3]Advanced Clinical Biosystems Research Institute, The Smidt Heart Institute, Cedars-Sinai Medical Center

[4]Department of Medicine, David Geffen School of Medicine, University of California Los Angeles

Abstract

Retinal degenerative diseases are some of the leading causes of blindness with few treatments. Various cell-based therapies have aimed to slow the progression of vision loss by preserving light-sensing photoreceptor cells. A subretinal injection of human neural progenitor cells (hNPCs) into the Royal College of Surgeons (RCS) rat model of retinal degeneration has aided in photoreceptor survival, though the mechanisms are mainly unknown. Identifying the retinal proteomic changes that occur following hNPC treatment will lead to better understanding of neuroprotection. To mimic the retinal environment following hNPC injection, a co-culture system of retinas and hNPCs was developed. Less cell death occurred in RCS retinal tissue co-cultured with hNPCs than in retinas cultured alone, suggesting that hNPCs provide retinal protection *in vitro*. Comparison of *ex vivo* and *in vivo* retinas identified NRF2-mediated oxidative response signaling as an hNPC-induced pathway. This is the first study to compare proteomic changes following treatment with hNPCs in both an *ex vivo* and *in vivo* environment, further allowing the use of *ex vivo* modeling for mechanisms of retinal preservation. Elucidation of the protein changes in the retina following hNPC treatment may lead to the discovery of mechanisms of photoreceptor survival and its therapeutic for clinical applications.

Corresponding Author: Shaomei Wang, Cedars-Sinai Medical Center, Board of Governors Regenerative Medicine Institute, 8700 Beverly Boulevard, Los Angeles, CA, 90048; Phone: (310)248-7970; shaomei.wang@cshs.org.

Authors' contributions

MKJ performed retinal *in vitro* and *in vivo* experiments, analyzed the data, and wrote the manuscript. BL performed experiments for the *in vivo* study. DZC assisted with experimental design and proteomic and bioinformatic analysis.WS prepared samples for proteomic analysis. AM performed the in vivo TUNEL study, AVL, CNS, and JEVE assisted with manuscript editing. SW assisted with experimental design, interpretation, editing of the manuscript and financial support. All authors read and approved the final manuscript.

Declarations:

Ethics approval and consent to participate

All animal research adhered to the Association for Research in Vision and Ophthalmology (ARVO) Statement for the Use of Animals in Ophthalmic and Vision research and was conducted with the approval of the Institutional Animal Care and Use Committee at Cedars-Sinai Medical Center.

Competing interests

The authors declare that they have no competing interests.

Author Manuscript Author Manuscript Author Manuscript Author Manuscript

Keywords

Human neural progenitor cells; neuroprotection; retinal degeneration; stem cells; transplantation

Introduction:

Retinal degenerative diseases (RDDs), such as age-related macular degeneration (AMD) and retinitis pigmentosa (RP), are characterized by progressive loss of vision and are leading causes of blindness in developed countries [1–3]. RDDs can be due to hereditary and/or lifestyle risk factors, but the overlying result is loss of the light sensitive photoreceptor cells within the retina, with no therapies to date to reverse the degeneration. Currently, stem cell-based therapies are being tested for clinical use and offer the potential to treat a number of RDDs [4–9]. One particular type of stem cell, human neural progenitor cells (hNPCs), is currently being tested for neuroprotective effects in other neurodegenerative disorders [10–13] and has similarly been shown to aid in visual function and photoreceptor preservation in animal models of retinal degeneration [6, 14–17]. In animal models of retinal degeneration, hNPCs are able to phagocytize photoreceptor outer segment *in vivo* [18, 19], exert a greater beneficial effect with expression of neurotrophic factors [14], and cause immunomodulatory effects on the host tissue [6]. However, many of the molecular changes that they elicit within the retinal tissue are unknown.

Whereas *in vivo* assays are the ideal model for studying retinal structure and degeneration, it can be technically challenging to identify key mechanistic aspects of the progression of disease and therapeutic interventions. The retina houses multiple types of cells that each play a role in visual function and determining the contributions of each cell type at specific time points *in vivo* can be analytically complicated. To this end, *in vitro* studies using retinal tissue explants have been developed for examining potential mechanisms that may mimic the *in vivo* environment. Such organotypic *ex vivo* systems also allow for more advanced manipulations and analyses, which can be difficult to interpret *in vivo*. Retinal explant techniques have been optimized for mouse, rat, rabbit, pig, and human studies [20–23]. Supplementation of media with serum or neurotrophic factors, has promoted survival of retinal explants [23–25], suggesting that exogenous components may alter the natural progression of development and cell death. Co-culture studies of wild-type retinal explant tissue and hNPCs have shown better retinal structure [26] and reduced microglial activation [27]. Artifacts of wild-type retinal degeneration *in vitro* may not represent disease modeling, and the use of inherent degenerative animal models could provide a more accurate picture of the progression of human retinal degeneration. One example is the Royal College of Surgeons (RCS) rat, which is a well-established model of retinitis pigmentosa [28, 29]. A mutation in the *Mertk* gene causes retinal pigment epithelial (RPE) cells to lose the ability to phagocytize shed outer segments from the adjacent photoreceptor cells, thus leading to an accumulation of undigested outer segments (called debris) in the subretinal space, photoreceptor degeneration, and vision loss. Adapting *ex vivo* techniques for the RCS rat and other retinal degenerate animal models could reveal neurodegenerative-specific mechanisms that are otherwise uncovered in wild-type experiments. Ultimately, this strategy

Author Manuscript Author Manuscript Author Manuscript Author Manuscript

could be useful in testing therapeutics for prolonging photoreceptor survival and thus be applied to *in vivo* studies of retinal degenerative diseases.

The proteomes of a number of human ocular tissues have been characterized, including the retina [30, 31]. Over 3,000 proteins were identified in the human retina with a number of those involved in the visual cycle and retinoid metabolism [32]. These protein signatures also allow for comparative analyses following retinal degeneration. Changes in the proteome have been detected in AMD patients [33–35], though this has typically been from blood samples that are more easily accessible than retina. Proteomic variations have been detected in rodent models of retinitis pigmentosa [36], AMD [37], and diabetic retinopathy [38, 39]. Moreover, protein changes have also been detected following gene therapy for Leber Congenital Amaurosis (LCA) specifically in proteins involved in neuroprotection and apoptosis [40], suggesting that proteomic analysis may elucidate some of the molecular mechanisms involved in treating retinal degeneration.

The therapeutic benefit of hNPCs for retinal degeneration can be detected morphologically and through visual function tests, but little is known about the molecular changes that occur. The main goal of this study was to establish an *ex vivo* co-culture model mimicking the *in vivo* environment following subretinal transplantation of hNPCs into retinal degenerate RCS rats. *Ex* vivo experiments suggested hNPCs aided in retinal survival, similar to the effects of subretinal injection of hNPCs in the RCS rat. Bioinformatic analysis identified proteomic changes in the presence of hNPCs, and specifically, one pathway, the NRF2-mediated oxidative stress response, was predicted to be highly activated in both *ex vivo* and *in vivo* RCS retinal tissue treated with hNPCs. These results suggest that similar hNPC-induced mechanisms occur both in culture and in the animal. Insight into the molecular changes following therapeutic intervention will elucidate mechanisms for retinal survival and may allow for more efficacious treatments using stem cells.

Materials and methods:

Derivation and maintenance of human neural progenitor cells (hNPCs)

hNPCs were provided by Dr. Clive Svendsen and their use has been previously described [6, 15, 17]. hNPCs were cultured as neurospheres in Stemline Neural Stem Cell Expansion Medium (Sigma-Aldrich, St. Louis, MO, USA) supplemented with 20 ng/ml epidermal growth factor (EGF; Sigma-Aldrich) and 10 ng/ml leukemia inhibitory factor (LIF; Millipore, Billerica, MA, USA) as previously described [11]. All experiments utilized hNPCs at passage 25, and were given fresh media every 3 to 4 days.

Co-culture conditions

hNPC neurospheres at passage 25 were dissociated into a single cell suspension by incubation at 37°C for 10 minutes with Accutase (Sigma-Aldrich) followed by two brief washes with media. Cells were counted using a hemocytometer, and 5×10^4 hNPCs were plated into each well of a 24-well plate (Greiner Bio-One, Monroe, NC, USA) and allowed to acclimate overnight in a 5% CO_2/37°C incubator. Eyes were enucleated from RCS rats at postnatal day 30 (P30) or day 60 (P60). Eyes were transported on ice from the vivarium to

Author Manuscript Author Manuscript Author Manuscript Author Manuscript

the laboratory in sterile 1X Dulbecco's phosphate buffered saline (ThermoFisher Scientific, Grand Island, NY, USA). The cornea and lens were dissected out and the eyecup was cut in half. Each half retina was placed on a nitrocellulose membrane, and the choroid was peeled from the neural retina. In *ex vivo* systems of wild-type animals, the RPE cell layer is typically attached to the neural retina upon dissection; however, the RPE cell layer becomes detached from the neural retinal layer in the degenerated RCS rat and very few pigmented cells remain attached to the neural retina. The nitrocellulose membrane and retina were trimmed to fit into a Thincert 0.4 μm pore translucent transwell chamber (Greiner Bio-One), and the pore size was chosen for ability of sharing media between the retina and hNPCs but would prohibit direct contact. placed into a 24-well plate with pre-warmed Stemline +EGF/LIF media and allowed to acclimate in an incubator at 5% CO_2/37°C for one hour. Following acclimation, half of the transwell inserts were cultured alone and the rest were co-cultured with hNPCs plated from the previous day. This study adhered to the Association for Research in Vision and Ophthalmology (ARVO) Statement for the Use of Animals in Ophthalmic and Vision research and was conducted with the approval of the Institutional Animal Care and Use Committee at Cedars-Sinai Medical Center.

In vitro sample preparation

hNPC, retina, and conditioned media samples were collected at the time of retinal dissection (day 0) and at 3 and 7 days in culture. For samples that were saved until 7 days, half of the media was removed at 3 days and the cultures received half fresh media. All samples were frozen at −80°C until processing. Media were collected from retinas cultured alone, hNPCs cultured alone, or hNPC and retinal co-cultures. For each type of sample, media were combined from 4 to 6 wells. To concentrate the proteins, each sample was added to a 10k Amicon Ultra-0.5 Centrifugal Filter Ultracel – 3K Device in a microcentrifuge tube (Millipore, Tullagreen, Co. Cork, Ireland). The filter columns were centrifuged per manufacturer's instructions for a final concentration factor of approximately 25- to 30-fold. hNPCs cultured alone or in co-culture with retinas were pooled for analysis from 4 to 6 replicate wells. Samples of retinas cultured alone or in co-culture with hNPCs were similarly pooled from 4 to 6 wells (Table 1).

Subretinal injection of hNPCs

hNPC neurospheres were dissociated into a single cell suspension by incubation at 37°C for 10 minutes with Accutase (Sigma-Aldrich) followed by incubation with trypsin inhibitor (Sigma-Aldrich) for 5 minutes and DNase (Sigma –Aldrich) for 10 minutes with gentle trituration in phosphate buffered saline (PBS, Thermo-Fisher Scientific, Grand Island, NY, USA). Cells were counted using a hemocytometer, and a dilution of 2×10^4 hNPCs/μL of balanced salt solution (BSS, Alcon, Fort Worth, TX) was prepared for each eye. RCS rats (n=3) at postnatal day 21 (P21) received a subretinal injection of hNPCs (RCS^{hNPCs}) at a dose of 4×10^4 per eye (2 μL total volume) through a glass micropipette as previously described [15]. The contralateral eye was left untreated, and untreated wild-type Long Evans (LE; n=3) rats were also used for comparison. Eyes were enucleated at age P60 and the neural retina was dissected away from the rest of the ocular tissue. For the hNPC injected eyes, retinas were cut in half and the area closest to the injection site was used for processing. The LE and untreated RCS samples were oriented in the same temporal to nasal

Author Manuscript Author Manuscript Author Manuscript Author Manuscript

direction as the previous samples and cut in half along the same hemisphere. All samples were stored at −80°C until further processing (Table 1).

Retinal sample preparation

Samples were lysed using 300 μL of lysis buffer (10 mM 4-(2-hydroxyethyl-1-piperazineethanesulfonic acid) (HEPES), 42 mM potassium chloride, 0.1 mM ethylenediaminetetraacetic acid (EDTA), 0.1 mM ethylene glycol-bis(β-aminoethyl ether)-N,N,N',N'-tetraacetic acid (EGTA), 1 mM dithiothreitol (DTT), 1x phosphatase inhibitor, and 1x protease inhibitor (Sigma-Aldrich)), homogenized, and sonicated. Further, 60 μL of 10% SDS was added to each sample and incubated for 10 minutes followed by centrifugation at 14,000 *g* for 45 minutes. The supernatant was collected, proteins were quantified using a NanoDrop One Analyzer (Thermo-Fisher), and samples were stored at −80°C.

Protein digestion

One aliquot of 50 μg of each sample type received 2 μLs of β-galactosidase (2mg/mL) as an internal control. Proteins were digested using the FASP Protein Digestion Kit (Expedeon, San Diego, CA, USA) per manufacturer's instructions. Desalting of the samples was then performed using an Oasis HLB 96-well plate 30 μm/5mg (Waters Corporation, Milford, MA, USA) attached to a vacuum. The plate was equilibrated with 700 μL of methanol and washed 3 times with 1 mL of 0.1% formic acid in water. Samples were prepared by adding 175 μL of 4% phosphoric acid to the plate, and vacuum filtered with 1 mL of 0.1% formic acid. Elution of the samples was performed with 600 μL of 80% hydrogen cyanide/0.1% formic acid in water. Peptide samples were extracted from the elution plate, put into new collection tubes and spun open in a Thermo Savant SPD2010 ° Concentrator (Thermo-Fisher) at 5.1 pressure and 45°C for approximately 6 hours.

Liquid chromatography (LC) mass spectrometry (MS)/MS

Trypsin digested retinal samples were analyzed by LC MS/MS using a Dionex Ultimate 3000 NanoLC connected to an Orbitrap Elite with an EasySpray ion source (Thermo Fisher). Peptides were loaded into the analytical column (PepMap RSLC C18 2μm, 100Å, 50μm i.d. x 15cm) with a flow rate of 300 nL/minute using a linear AB gradient (2 to 25% A for 185 minutes and 25–90% B for 5 minutes) followed by isocratic hold at 90% for 5 minutes and re-equilibrating at 2% A for 10 minutes. The temperature for both columns was 40°C, and the Nano-source capillary temperature was set to 275°C with a spray voltage at 2 kilovolts (kV). The Orbitrap Elite captured MS1 scans with a resolution of 60,000 full width at half maximum (FWHM) with an automatic gain control (AGC) target of 1×10^6 ions with a maximum of 500 milliseconds. MS2 spectra were then collected for the top 15 ions from each MS1 scan with a target of 1×10^4 ions, accumulation time of 100 milliseconds, and an isolation width of 2 Dalton (Da). The normalized collision energy was set at 35%, and one microscan was obtained for each spectrum.

Author Manuscript Author Manuscript Author Manuscript Author Manuscript

Bioinformatic analyses

All of the processed proteomics samples were Raw MS files were first converted to mzXML files using MSConvert [41]. Data files from each sample were searched against the human (media) or rat (retinas) protein database by Trans Proteomic Pipeline Software [42, 43]. The interaction files prepared from Trans Proteomic Pipeline were then input into Skyline daily software [44]. Protein identification was based on 2 or more peptide matches with a false discovery rate < 5%. Relative abundance values for proteins were calculated from peak areas using the Skyline daily MPPReport plugin. Relative abundance values were $\log_2$ transformed, normalization was performed by median polish, and the ratios between the averaged $\log_2$ relative abundance values were calculated and presented as fold change values between the samples. Hierarchical cluster analysis was performed using BioVinci Software (Bioturing, San Diego, CA, USA). Pathway analysis of the protein datasets from all of the samples (media and retinas) were input into the Ingenuity Pathway Analysis (IPA) Fall 2016 Release Software (QIAGEN, Redwood City, CA, USA; www.qiagen.com/ingenuity). Significantly affected canonical pathways and biofunctional properties were identified by –log Benjamini-Hochberg Multiple Testing Correction *p*-value statistics (significant at >1.3) and an activation *z*-score ≥2 or ≤−2.

Retinal cryosections

For the *in vitro* experiments, 7-day old cultured retinas were fixed with 4% paraformaldehyde (PFA) overnight at 4°C followed by 10%, 20%, and 30% sucrose solutions in 1X PBS for 1 hour each at room temperature, embedded in optimum cutting temperature compound (OCT; Sakura Finetek, Torrance, CA, USA), and stored at −80°C. Horizontal sections at were cut at 10 μm on a Leica CM1850 cryostat microtome (Leica Biosystems, Nussloch, Germany). Four sections at 50 μm distance were collected in five series and stored at −20°C. For the *in vivo* experiments, eyes were prepared as above with the exception of fixation for 1 hour at room temperature with 4% PFA. Retinal sections from the *in vivo* experiments were stained with cresyl violet dye for histological analysis and imaged with a Leica DM6000B microscope (Leica Microsystems, Wetzlar, Germany).

Imaging and quantification of dead, retinal cells

To identify dead retinal cells, terminal deoxynucleotidyl transferase dUTP Nick-End labeling (TUNEL) assay was performed using the TUNEL Apoptosis Detection Kit (Millipore, Darmstadt, Germany) per manufacturer's instructions. Sections were washed with 10X phosphate buffered saline (PBS) for 30 minutes at 37°C followed by incubation for 15 minutes at 37°C with proteinase K solution and four more washes with 10x PBS for 2 minutes each. For a positive control, one slide was incubated with DNase I (1 μg/mL) for 60 minutes at 37°C followed by a 15-minute wash with 10X PBS. All sections were then equilibrated with terminal deoxynucleotidyl transferase (TdT) buffer for 5 minutes, and incubated with TdT end-labeling cocktail (TdT buffer, Biotin-2'-deoxyuridine 5'-triphosphate (dUTP), and TdT at a ratio of 90:5:5, respectively) for 60 minutes at 37°C. To stop the reaction, sections were immersed in 1X TB buffer for 5 minutes at room temperature and washed with PBS 4 times for 2 minutes each. Blocking buffer was added to each section and incubated at room temperature for 20 minutes, followed by incubation for

Author Manuscript Author Manuscript Author Manuscript Author Manuscript

30 minutes at 37°C in the dark with Avidin-fluorescein isothiocyanate [45] solution. All sections were washed with PBS 2 times for 15 minutes in the dark at room temperature, counterstained with 4',6-diamidino-2-phenylindole, dihydrochloride (DAPI) for 20 minutes in the dark, and mounted with a coverslip. Sections were imaged in a fluorescent microscope Leica microscope DM6000B. For the *ex vivo* experiments, one slide contained 4 sections at 50 μm distance between the sections from each RCS sample with or without hNPC co-culture. $TUNEL^+$ cells were counted using the cell counting plugin from ImageJ. The percentage of $TUNEL^+$ cells were calculated from averages of each $TUNEL^+$ section divided by the average of total number of $DAPI^+$ cells and multiplied by 100. For *in vivo* retinal photoreceptor cell death, TUNEL assay and counterstain with DAPI were imaged. In the hNPC-grafted retinas, 3 images were taken at an area close to the injection site with 5–8 layers of preserved photoreceptors. In the BSS-treated retinas, 3 images were taken close to the injection sites. Numbers of TUNEL-positive cells in the outer nuclear layer (ONL) were counted in 3 images/sections, 9 sections/eye in 3 eyes from each of the groups. Student's t test was used to statistically compare the results.

Results:

hNPCs promote retinal survival in vitro

To determine if hNPCs can provide the same benefit *in vitro*, a co-culture assay was performed. Retinal tissue from RCS rats was dissected from two stages of degeneration. At P30, retinal degeneration is classified as an early stage, whereas P60 retina is considered middle stage degeneration. Retinal tissue was cultured for up to 7 days, and then subjected to proteomic analysis. A total of 585 proteins were identified (Supplemental Table 1). The analysis of protein profiles indicated differences in activation of cell survival and cell death (Figure 1A). P60 retinas at both 3 and 7 days in culture showed activation of cell death and inhibition of cell survival pathways, whereas P30 retina had significance only at 7 days in culture. To determine if hNPCs induce retinal survival *in vitro*, P30 and P60 retinas were co-cultured with hNPCs and proteomic analysis was conducted. A total of 578 proteins were identified in common in the co-cultured retinas (Supplemental Table 2), and functional analysis was performed (Figure 1B). Age P30 retina co-cultured with hNPCs for 7 days had activation of cell survival and inhibition of cell death pathways, suggesting that hNPCs impact retinal cell survival and death pathways at the early stages of degeneration. No significant difference was detected at 7 days with late stage degenerative retinas (P60) co-cultured with hNPCs. To validate the proteomic differences in cell survival in early stage degeneration, an apoptosis assay was performed on cultured retinal tissue (Figure 1C). At 7 days in culture, the P30 retina had a high percentage of apoptotic cells; however, P30 retinas co-cultured with hNPCs for the same number of days had a significant decrease in the percent of TUNEL-positive dead cells ($p < 0.01$). These findings indicate that hNPCs aid in retinal survival when co-cultured with early stage degenerating retinas.

Pathway analysis of co-cultured retinas

Since age P30 retina at 7 days in co-culture with hNPCs had significant differences in cell survival, the bioinformatic analyses were focused on this age and time point. To identify pathways that are differentially regulated in co-cultured retinas, the protein profiles were

Author Manuscript Author Manuscript Author Manuscript Author Manuscript

input into Ingenuity Pathway Analysis (IPA) software. A total of 8 canonical pathways were significantly predicted to be activated in co-cultured P30 day 7 retinas as compared to P30 day 7 retinas cultured alone (Figure 1D). These pathways included NRF2-mediated oxidative stress response (-log Benjamini-Hochberg *p*-value 4.7), p70S6K signaling (-log Benjamini-Hochberg *p*-value 4.2), aldosterone signaling in epithelial cells (-log Benjamini-Hochberg *p*-value 3.6), CREB signaling in neurons (-log Benjamini-Hochberg *p*-value 1.9), nitric oxide signaling (-log Benjamini-Hochberg *p*-value 1.8), thrombin signaling (-log Benjamini-Hochberg *p*-value 1.6), synaptic long term potentiation (-log Benjamini-Hochberg *p*-value1.6), and IL-1 signaling (-log Benjamini-Hochberg *p*-value 1.4). To identify molecules that could potentially regulate these pathways, significantly predicted upstream regulators were also identified (Figure 1E). Upstream regulator analysis is based on the expression of detected proteins within the dataset, which then predicts genes/proteins upstream of these proteins that may regulate their expression. The regulator with the most significant activation was NFE2L2, which is also known as NRF2, and was also identified in the canonical pathway analysis (Figure 1D), suggesting that NRF2-mediated oxidative stress response is one of the highly activated pathways in retinas co-cultured with hNPCs.

In vitro hNPC secreted factors

To identify proteins in co-cultured media, proteomic analysis was also performed. Media were collected from hNPCs cultured alone and from co-cultures of age P30 retinas with hNPCs. Proteomic analysis detected a total of 551 proteins in all media (Supplemental Table 3). *In silico* functional analysis of proteins identified significant differences in cell survival and cell death in co-cultured media from the RCS age P30 retinas at 7 days in culture (Figure 2A, Supplemental Table 4). Statistical significance was detected for cell death (activation z-score −6.3) and cell survival (activation z-score 5.5), suggesting that proteins in the co-cultured media are inhibiting cell death and promoting cell survival at 7 days in culture more than at 3 days in culture with P30 retina. Since the co-culture media showed more activation of pro-survival and inhibition of cell death, the next step was to identify the pathways that may be involved in aiding in these processes. Canonical pathways were identified in co-cultured media from hNPCs and P30 retinas at 7 days in culture (Figure 2B). Of the 14 significantly changed pathways, 13 were predicted to be upregulated (actin cytoskeleton signaling, RhoA signaling, EIF2 signaling, signaling by Rho family GTPases, NRF2-mediated oxidative stress response, integrin signaling, 14-3-3-mediated signaling, regulation of actin-based motility by Rho, leukocyte extravasation signaling, PI3K/AKT signaling, remodeling of epithelial adherens junctions, protein kinase A signaling, ILK signaling, and VEGF signaling) with 1 pathway (HIPPO signaling) inhibited. To further distinguish pathways that may be involved, upstream regulators were determined by IPA (Qiagen) software. A total of 143 regulators were identified (Supplemental Table 5) and the top 10 most highly activated and inhibited are shown (Figure 2C). The most significantly predicted activated upstream regulator was NFE2L2/NRF2. The NRF2-mediated oxidative stress response was also identified as one of the most highly activated canonical pathways (Figure 2B), suggesting that it may be regulated by secreted factors from the hNPCs. NRF2-mediated oxidative stress response was also detected as the most significantly activated in *ex vivo* retinal tissue (Figure 1) further implicating this pathway as an important regulator hNPC-dependent in co-cultured retinal tissue.

Author Manuscript Author Manuscript Author Manuscript Author Manuscript

Proteomic comparison of retinal samples

At the histological level, P60 LE rats have approximately 10 layers of photoreceptor cells in the outer nuclear layer (ONL; Figure 3A). Age-matched RCS rats have undergone photoreceptor degeneration and have 2 to 3 layers of photoreceptors (Figure 3B). Conversely, RCS^{hNPCs} have approximately 5 to 6 layers of photoreceptor cells (Figure 3C), and the photoreceptor survival directly correlates with the presence of hNPCs. Furthermore, TUNEL assay was performed on RCS and RCS^{hNPCs} retinas and showed a significant decrease in the number of apoptotic cells with the presence of hNPCs (Figure 3D). To determine if these morphological differences in photoreceptor survival can be detected at the protein level, proteomic analysis was performed. A total of 434 proteins were identified in common between the retinal samples (Supplemental Table 6). To identify if differences in cell survival can be detected at the protein level, *in silico* functional analysis was performed. Cell survival was shown to be inhibited in RCS samples as compared to wild-type LE (Figure 3D, left), suggesting that there is less photoreceptor survival detected in both of the RCS samples regardless of treatment. However, RCS^{hNPCs} as compared to untreated RCS showed an activation in cell survival (Figure 3D, left), suggesting that cells survive better in RCS retinas treated with hNPCs. Similarly, cell death was activated in RCS samples as compared to LE; however, RCS^{hNPCs} showed inhibition of cell death as compared to untreated RCS (Figure 3D, right). These results suggest that RCS^{hNPCs} have more cell survival relative to RCS, which is similar to what is detected at the morphological level.

Putative mechanisms of photoreceptor survival in vivo

To identify mechanisms that may be aiding in photoreceptor survival, further pathway analysis was performed on the data obtained from the *in vivo* retinal samples. Nine pathways were found to be significant in the comparisons between the samples (Figure 5). Many of the pathways were changed in the RCS samples as compared to LE, but it was reversed when RCS^{hNPCs} were compared to untreated RCS. These pathways included 14-3-3 mediated signaling, ERK5 signaling, LXR/RXR activation, NRF2-mediated oxidative response, PI3K/AKT signaling, and protein kinase A signaling (Figure 4A, C, E, F, H, and I). Similarly, HIPPO pathway was predicted to be activated in RCS samples yet inhibited when RCS^{hNPCs} was compared with RCS (Figure 4D). Collectively, these pathways indicate that there are proteomic and signaling changes that occur following injection of hNPCs. Two pathways, the acute phase response and p70S6K signaling, were found to be inhibited in the RCS samples as compared to the LE samples (Figure 4B and G) and were not significantly different between the two RCS samples, suggesting that there is no effect with hNPCs on certain pathways. Overall, multiple pathways may play roles in hNPC-induced photoreceptor survival.

Though a number of signaling pathways were uniquely identified in each of the experiments, only one canonical pathway was found in common between the co-cultured *in vitro* and *in vivo* proteomic analysis, suggesting that similar mechanisms of photoreceptor survival may be occurring in both situations. To determine if common proteins are expressed within the retina in the *in vitro* and *in vivo* experiments, downstream proteins of the NRF2-mediated oxidative stress response from both experiments was compared. P30 retinas cultured alone for 7 days and untreated RCS retinas expressed downregulation of proteins downstream of

Author Manuscript Author Manuscript Author Manuscript Author Manuscript

the NRF2-mediated oxidative stress response (Figure 5). P30 retinas co-cultured with hNPCs for 7 days and RCS^{hNPCs} showed upregulation of many of these same proteins, and more closely aligned with the expression profiles of wild-type LE retina (Figure 5). This suggests that there is an increase in NRF2-mediated oxidative stress response signaling with hNPC treatment, indicating that similar mechanisms operate in both the *in vitro* and *in vivo* retinas in the presence of hNPCs.

Discussion:

Our lab and others have shown that hNPCs aid in photoreceptor survival *in vivo*, and the results of this study indicate that there are significant protein changes occurring upon treatment of RCS rat retinas with hNPCs that delay retinal degeneration. The canonical pathways identified by proteomic analysis may be further investigated to determine their involvement in hNPC-induced photoreceptor survival. Specifically, the NRF2-mediated oxidative stress response was not only activated in RCS^{hNPCs} retinas but was also one of the main activated pathways possibly contributing to *ex vivo* retinal survival. These data suggest that similar hNPC-induced survival mechanisms occur both *ex vivo* and *in vivo*, and this knowledge could be used to screen therapeutic agents *in vitro* for future translational applications.

Putative pro-survival mechanisms

As shown with both *ex vivo* and *in vivo* analyses, numerous protein expression changes occur upon treatment with hNPCs. Bioinformatic analysis of proteins expressed in retinal tissue identified hNPC-induced signaling pathways and upstream regulators that may play roles in photoreceptor survival. One pathway, p70S6k signaling, was activated in co-cultured retinas yet deactivated in the *in vivo* untreated and hNPC-treated RCS samples as compared to LE (Figures 2A and4G). This pathway is part of the PI3K/AKT signaling mechanism for apoptosis, cell survival, cell growth, protein translation, and autophagy [46, 47]. Inhibition of p70S6K has been shown to prevent retinal neuronal cell survival, whereas overexpression enhances insulin-dependent survival [48]. In our study, inhibition of p70S6K in the *in vivo* RCS samples suggests that retinal cell death is occurring, even with hNPC treatment. The hNPCs are slowing down the degeneration process [6, 14–17]; however, a higher dose or combined treatment such as improving host degenerative retinal environment may be needed to protect the retina more efficiently. Conversely, PI3K/AKT signaling was activated in RCS^{hNPCS} as compared to untreated RCS, suggesting that the other pro-survival mechanisms may be triggered in tandem. In addition, the *ex vivo* co-cultured retinas activated p70S6K signaling, indicating overlap of identified pathways and potential similar mechanisms of survival.

Four additional pathways were found to be deactivated in both RCS samples compared to LE but were activated in RCS^{hNPCs} compared to RCS (Figure 4A, C, E, F, and I). The first pathway, 14-3-3 mediated signaling, controls a range of signal transduction pathways and anti-apoptotic activity [49]. 14-3-3 proteins are involved in the pathogenesis of neurodegenerative diseases, such as Parkinson's disease, Alzheimer's disease, and amyotrophic lateral sclerosis (ALS), and may play a role in neuroprotection [50]. The second

Author Manuscript Author Manuscript Author Manuscript Author Manuscript

pathway, ERK5 signaling, is stimulated in response to cell stress, mediates neuronal survival [51], and is activated in the retina upon neurotrophic stimulation [52]. Third, the LXR/RXR activation pathway was also predicted to be activated in RCS retina treated with hNPCs. LXRs (liver X receptors) are transcription factors that regulate genes involved in lipid homeostasis, immunity and neurological functions [53, 54], and LXR agonists have been shown to reduce the severity of wet AMD by decreasing macrophage activation [55]. Additionally, RXRs (retinoid X receptors) regulate expression of apoptotic proteins, and specifically activate antioxidant mechanisms for photoreceptor survival [56] and protective effects for RPE cells [57]. The fourth pathway, protein kinase A signaling, participates in retinal circuitry and activity as part of a calcium-dependent second messenger cascade [58]. Similarly, one pathway, HIPPO signaling, was activated in both of the RCS samples as compared to LE but was inhibited in RCS^{hNPCs} compared to RCS (Figure 4D). HIPPO signaling regulates cell survival, retinogenesis, and photoreceptor cell differentiation [59, 60]. Feasibly, numerous hNPC-induced signaling mechanisms may be interacting and working in concert with each other to aid in photoreceptor survival and neuroprotection.

NRF2-mediated oxidative stress response in retinal degeneration

The NRF2-mediated oxidative stress response pathway was also inhibited in both RCS samples (*in vitro* and *in vivo*) as compared to LE but was activated in RCS^{hNPCs}. The NRF2-mediated oxidative response regulates tolerance to oxidative stress [33]. In an unstressed state, the proteins Nrf2 and Keap1 are bound and localized within the cytoplasm. Following endoplasmic reticulum (ER) stress, Nrf2 becomes phosphorylated, dissociates from Keap1, and translocates to the nucleus. This results in an increase in Nrf2-dependent transcription of antioxidant response genes, thus promoting cell survival and redox homeostasis [61]. NRF2 regulates the antioxidant defense against oxidative damage and acts as a neuroprotectant in neurodegenerative diseases [62]. Elements of the NRF2 signaling pathway have been used as therapeutic targets for neurodegenerative diseases, such as Alzheimer's [63], Parkinson's [64], and Huntington's disease [65], and similar effects are observed in the retina. Oxidative stress is considered one of the main pathological factors in AMD [66]. Decreasing the amount of oxidative stress in retinal pigment epithelial cells resulted in RPE cell survival [67], suggesting that oxidative stress could be targeted as a potential treatment for AMD and other retinal degenerative diseases. Additionally, delivery of NRF2 protects photoreceptors from oxidative stress [68]. Impaired NRF2 signaling has been implicated in RPE damage [69], suggesting that NRF2 may be necessary for retinal neuroprotection and could be used as a retinal target for therapeutics. Interestingly, the Nrf2 protein itself was not detected in either the *in vitro* or *in vivo* proteomic datasets. This could be due to either low abundance of the protein or technical constraints. The basal level of NRF2 is relatively low within cells, as it is consistently targeted for degradation and has a half-life of 10 to 20 minutes [70, 71]. Mass spectrometry would detect the most abundant proteins within a sample, whereas lower abundance proteins are typically not identified unless an enrichment protocol or deletion of higher abundance proteins is performed [72, 73]. Further proteomic analysis, such as Western blot, immunostaining, or data-dependent acquisition mass spectrometry, may be able to detect NRF2 and/or where within the retina it is located. The findings from this study further suggest that cellular stress plays a role in retinal degeneration and that the hNPCs react by upregulating pathways involved in the stress response. Furthermore, the NRF2-mediated

Author Manuscript Author Manuscript Author Manuscript Author Manuscript

oxidative response could be a potential communicative element between the hNPCs and ailing retina and should be further investigated in the *in vivo* setting for validation of its involvement.

Limitations of retinal proteomic analysis

Some difficulties may potentially arise with the use of proteomics for detecting retinal proteins. The first is based on technical sensitivity, as low abundance proteins are difficult to detect and not all of the proteins have been identified. It is estimated that approximately 80% of the proteins in humans have been detected with high-confidence, but the remaining 20% of proteins have not been identifiable with current experimental methods [74, 75]. Additionally, protein and transcript levels do not always overlap so transcriptomic and proteomic analyses may not be directly comparable. Retinal tissue used for both microarray and proteomic experiments had <10% overlap of significantly identified genes and proteins [40]. Further, numerous cell types reside within the retina and a global view of all retinal proteins may not accurately identify cell-specific mechanisms. This study is the first step in elucidating and comparing some of the mechanisms in both an *in vitro* and *in vivo* environment; however, further proteomic analysis could be performed with particular cell types, such as photoreceptors and retinal supporting Müller glia.

The mass spectrometry proteomics data have been deposited to the ProteomeXchange Consortium via the PRIDE [76] partner repository with the dataset identifier PXD011491.

Supplementary Material

Refer to Web version on PubMed Central for supplementary material.

Acknowledgements:

The authors would like to thank Aaron Robinson from the Department of Biomedical Sciences at Cedars-Sinai Medical Center for his aid in proteomic analyses. The authors would also like to express gratitude to the Advanced Clinical Biosystems Research Institute at Cedars-Sinai Medical Center for mass spectrometry sample preparation and proteomic analysis.

Support for this study was provided by the National Eye Institute (R01EY020488), California Institute for Regenerative Medicine (LSP1–08235), and Cedars-Sinai Medical Center Board of Governors Regenerative Medicine Institute.

Abbreviations:

AMD	Age-related macular degeneration
ARVO	Association for Research in Vision and Ophthalmology
BSS	balanced salt solution
EGF	epidermal growth factor
hNPCs	human neural progenitor cell
IPA	Ingenuity Pathway Analysis

Author Manuscript Author Manuscript Author Manuscript Author Manuscript

LIF	leukemia inhibitory factor
LCA	Leber Congenital Amaurosis
LC MS	Liquid chromatography mass spectrometry
LXR	Liver X receptor
LE	Long Evans
NRF2	Nuclear factor erythroid-derived 2
ONL	outer nuclear layer
RDDs	retinal degenerative diseases
RP	retinitis pigmentosa
RCS	Royal College of Surgeons
RCS^{hNPCs}	Royal College of Surgeons rats injected with human neural progenitor cells

References

[1]. Klein R, Ophthalmic Epidemiol 2007, 14.

[2]. Sorrentino FS, Gallenga CE, Bonifazzi C, Perri P, Eye (Lond) 2016, 30.

[3]. Lim LS, Mitchell P, Seddon JM, Holz FG, Wong TY, Lancet 2012, 379.

[4]. Ehmann D, Shahlaee A, Ho AC, Curr Opin Ophthalmol 2016, 27.

[5]. Garcia JM, Mendonca L, Brant R, Abud M, Regatieri C, Diniz B, World J Stem Cells 2015, 7.

[6]. Jones MK, Lu B, Saghizadeh M, Wang S, Mol Vis 2016, 22.

[7]. Marchetti V, Krohne TU, Friedlander DF, Friedlander M, J Clin Invest 2010, 120. [PubMed: 21123944]

[8]. Trounson A, DeWitt ND, Nat Rev Mol Cell Biol 2016, 17.

[9]. Zarbin M, Trends Mol Med 2016, 22.

[10]. Blurton-Jones M, Kitazawa M, Martinez-Coria H, Castello NA, Muller FJ, Loring JF, Yamasaki TR, Poon WW, Green KN, LaFerla FM, Proc Natl Acad Sci U S A 2009, 106.

[11]. Goldberg NRS, Marsh SE, Ochaba J, Shelley BC, Davtyan H, Thompson LM, Steffan JS, Svendsen CN, Blurton-Jones M, Stem Cells Transl Med 2017, 6. [PubMed: 29105375]

[12]. Hampton DW, Webber DJ, Bilican B, Goedert M, Spillantini MG, Chandran S, J Neurosci 2010, 30.

[13]. Mendes-Pinheiro B, Teixeira FG, Anjo SI, Manadas B, Behie LA, Salgado AJ, Stem Cells Transl Med 2018.

[14]. Gamm DM, Wang S, Lu B, Girman S, Holmes T, Bischoff N, Shearer RL, Sauve Y, Capowski E, Svendsen CN, Lund RD, PLoS ONE 2007, 2.

[15]. Y. LLu B, Tsai Y, Girman S, Adamus G, Jones MK, Shelley B, Svendsen CN, Wang S, Trans. Vis. Sci. Tech 2015, 4.

[16]. McGill TJ, Cottam B, Lu B, Wang S, Girman S, Tian C, Huhn SL, Lund RD, Capela A, Eur J Neurosci 2012, 35. [PubMed: 23121157]

[17]. Wang S, Girman S, Lu B, Bischoff N, Holmes T, Shearer R, Wright LS, Svendsen CN, Gamm DM, Lund RD, Invest Ophthalmol Vis Sci 2008, 49. [PubMed: 18172074]

[18]. Cuenca N, Fernandez-Sanchez L, McGill TJ, Lu B, Wang S, Lund R, Huhn S, Capela A, Invest Ophthalmol Vis Sci 2013, 54.

Author Manuscript Author Manuscript Author Manuscript Author Manuscript

[19]. Tsai YC LB, Bakondi A, Girman S, Sahabian A, Sareen D, Svendsen CN and Wang S, Stem Cells 2015, 33, 2537. [PubMed: 25869002]

[20]. Caffe AR, Ahuja P, Holmqvist B, Azadi S, Forsell J, Holmqvist I, Soderpalm AK, van Veen T, J Chem Neuroanat 2001, 22.

[21]. Di Lauro S, Rodriguez-Crespo D, Gayoso MJ, Garcia-Gutierrez MT, Pastor JC, Srivastava GK, Fernandez-Bueno I, Mol Vis 2016, 22.

[22]. Marita KG, J Ophthalmic Vis Res 2011, 6.

[23]. Moritoh S, Tanaka KF, Jouhou H, Ikenaka K, Koizumi A, PLoS One 2010, 5.

[24]. Bull ND, Johnson TV, Welsapar G, DeKorver NW, Tomarev SI, Martin KR, Invest Ophthalmol Vis Sci 2011, 52.

[25]. Pinzon-Duarte G, Arango-Gonzalez B, Guenther E, Kohler K, Eur J Neurosci 2004, 19.

[26]. Mollick T, Mohlin C, Johansson K, Brain Res 2016, 1646.

[27]. Mohlin C, Liljekvist-Soltic I, Johansson K, J Neural Eng 2011, 8.

[28]. D'Cruz PM, Yasumura D, Weir J, Matthes MT, Abderrahim H, LaVail MM, Vollrath D, Hum Mol Genet 2000, 9.

[29]. Vollrath D, Feng W, Duncan JL, Yasumura D, D'Cruz PM, Chappelow A, Matthes MT, Kay MA, LaVail MM, Proc Natl Acad Sci U S A 2001, 98.

[30]. Semba RD, Enghild JJ, Venkatraman V, Dyrlund TF, Van Eyk JE, Proteomics 2013, 13.

[31]. Velez G, Machlab DA, Tang PH, Sun Y, Tsang SH, Bassuk AG, Mahajan VB, PLoS One 2018, 13.

[32]. Zhang P, Dufresne C, Turner R, Ferri S, Venkatraman V, Karani R, Lutty GA, Van Eyk JE, Semba RD, Proteomics 2015, 15.

[33]. Gu J, Pauer GJ, Yue X, Narendra U, Sturgill GM, Bena J, Gu X, Peachey NS, Salomon RG, Hagstrom SA, Crabb JW, Adv Exp Med Biol 2010, 664.

[34]. Kim HJ, Ahn SJ, Woo SJ, Hong HK, Suh EJ, Ahn J, Park JH, Ryoo NK, Lee JE, Kim KW, Park KH, Lee C, Sci Rep 2016, 6. [PubMed: 28442741]

[35]. Koss MJ, Hoffmann J, Nguyen N, Pfister M, Mischak H, Mullen W, Husi H, Rejdak R, Koch F, Jankowski J, Krueger K, Bertelmann T, Klein J, Schanstra JP, Siwy J, PLoS One 2014, 9.

[36]. Cavusoglu N, Thierse D, Mohand-Said S, Chalmel F, Poch O, Van-Dorsselaer A, Sahel JA, Leveillard T, Mol Cell Proteomics 2003, 2. [PubMed: 12601077]

[37]. Kraljevic Pavelic S, Klobucar M, Sedic M, Micek V, Gehrig P, Grossman J, Pavelic K, Vojnikovic B, Biochim Biophys Acta 2015, 1852.

[38]. Quin G, Len AC, Billson FA, Gillies MC, Proteomics 2007, 7.

[39]. VanGuilder HD, Bixler GV, Kutzler L, Brucklacher RM, Bronson SK, Kimball SR, Freeman WM, PLoS One 2011, 6.

[40]. Zheng Q, Ren Y, Tzekov R, Zhang Y, Chen B, Hou J, Zhao C, Zhu J, Zhang Y, Dai X, Ma S, Li J, Pang J, Qu J, Li W, PLoS One 2012, 7.

[41]. Chambers MC, Maclean B, Burke R, Amodei D, Ruderman DL, Neumann S, Gatto L, Fischer B, Pratt B, Egertson J, Hoff K, Kessner D, Tasman N, Shulman N, Frewen B, Baker TA, Brusniak MY, Paulse C, Creasy D, Flashner L, Kani K, Moulding C, Seymour SL, Nuwaysir LM, Lefebvre B, Kuhlmann F, Roark J, Rainer P, Detlev S, Hemenway T, Huhmer A, Langridge J, Connolly B, Chadick T, Holly K, Eckels J, Deutsch EW, Moritz RL, Katz JE, Agus DB, MacCoss M, Tabb DL, Mallick P, Nat Biotechnol 2012, 30. [PubMed: 22231088]

[42]. Deutsch EW, Mendoza L, Shteynberg D, Farrah T, Lam H, Tasman N, Sun Z, Nilsson E, Pratt B, Prazen B, Eng JK, Martin DB, Nesvizhskii AI, Aebersold R, Proteomics 2010, 10.

[43]. Keller A, Eng J, Zhang N, Li XJ, Aebersold R, Mol Syst Biol 2005, 1.

[44]. MacLean B, Tomazela DM, Shulman N, Chambers M, Finney GL, Frewen B, Kern R, Tabb DL, Liebler DC, MacCoss MJ, Bioinformatics 2010, 26. [PubMed: 20070902]

[45]. Goldstein LE, Muffat JA, Cherny RA, Moir RD, Ericsson MH, Huang X, Mavros C, Coccia JA, Faget KY, Fitch KA, Masters CL, Tanzi RE, Chylack LT, Jr., Bush AI, Lancet 2003, 361. [PubMed: 12573369]

[46]. Cai N, Dai SD, Liu NN, Liu LM, Zhao N, Chen L, Int J Ophthalmol 2012, 5.

Author Manuscript Author Manuscript Author Manuscript Author Manuscript

[47]. Huang SP, Chien JY, Tsai RK, Dis Model Mech 2015, 8.

[48]. Wu X, Reiter CE, Antonetti DA, Kimball SR, Jefferson LS, Gardner TW, J Biol Chem 2004, 279.

[49]. Yang X, Luo C, Cai J, Pierce WM, Tezel G, Invest Ophthalmol Vis Sci 2008, 49. [PubMed: 18172074]

[50]. Shimada T, Fournier AE, Yamagata K, Biomed Res Int 2013, 2013.

[51]. Watson FL, Heerssen HM, Bhattacharyya A, Klesse L, Lin MZ, Segal RA, Nat Neurosci 2001, 4.

[52]. van Oterendorp C, Sgouris S, Schallner N, Biermann J, Lagreze WA, Invest Ophthalmol Vis Sci 2014, 55. [PubMed: 24222300]

[53]. Choudhary M, Malek G, Adv Exp Med Biol 2016, 854.

[54]. Hong C, Tontonoz P, Nat Rev Drug Discov 2014, 13. [PubMed: 24378792]

[55]. Sene A, Khan AA, Cox D, Nakamura RE, Santeford A, Kim BM, Sidhu R, Onken MD, Harbour JW, Hagbi-Levi S, Chowers I, Edwards PA, Baldan A, Parks JS, Ory DS, Apte RS, Cell Metab 2013, 17.

[56]. German OL, Agnolazza DL, Politi LE, Rotstein NP, Photochem Photobiol Sci 2015, 14.

[57]. Ayala-Pena VB, Pilotti F, Volonte Y, Rotstein NP, Politi LE, German OL, Biochim Biophys Acta 2016, 1863.

[58]. Dunn TA, Wang CT, Colicos MA, Zaccolo M, DiPilato LM, Zhang J, Tsien RY, Feller MB, J Neurosci 2006, 26.

[59]. Asaoka Y, Hata S, Namae M, Furutani-Seiki M, Nishina H, PLoS One 2014, 9.

[60]. Wittkorn E, Sarkar A, Garcia K, Kango-Singh M, Singh A, Development 2015, 142.

[61]. Darling NJ, Cook SJ, Biochim Biophys Acta 2014, 1843.

[62]. Gan L, Johnson JA, Biochim Biophys Acta 2014, 1842.

[63]. Kim HV, Kim HY, Ehrlich HY, Choi SY, Kim DJ, Kim Y, Amyloid 2013, 20.

[64]. He Q, Song N, Jia F, Xu H, Yu X, Xie J, Jiang H, Int J Biochem Cell Biol 2013, 45.

[65]. Stack C, Ho D, Wille E, Calingasan NY, Williams C, Liby K, Sporn M, Dumont M, Beal MF, Free Radic Biol Med 2010, 49.

[66]. Shaw PX, Stiles T, Douglas C, Ho D, Fan W, Du H, Xiao X, AIMS Mol Sci 2016, 3.

[67]. Zhu Y, Zhao KK, Tong Y, Zhou YL, Wang YX, Zhao PQ, Wang ZY, Sci Rep 2016, 6. [PubMed: 28442741]

[68]. Xiong W, MacColl Garfinkel AE, Li Y, Benowitz LI, Cepko CL, J Clin Invest 2015, 125.

[69]. Sachdeva MM, Cano M, Handa JT, Exp Eye Res 2014, 119.

[70]. Bryan HK, Olayanju A, Goldring CE, Park BK, Biochem Pharmacol 2013, 85.

[71]. Itoh K, Wakabayashi N, Katoh Y, Ishii T, O'Connor T, Yamamoto M, Genes Cells 2003, 8.

[72]. Gillette MA, Carr SA, Nat Methods 2013, 10.

[73]. Millioni R, Tolin S, Puricelli L, Sbrignadello S, Fadini GP, Tessari P, Arrigoni G, PLoS One 2011, 6.

[74]. Baker MS, Ahn SB, Mohamedali A, Islam MT, Cantor D, Verhaert PD, Fanayan S, Sharma S, Nice EC, Connor M, Ranganathan S, Nat Commun 2017, 8. [PubMed: 28364116]

[75]. Lane L, Bairoch A, Beavis RC, Deutsch EW, Gaudet P, Lundberg E, Omenn GS, J Proteome Res 2014, 13.

[76]. Vizcaino JA, Csordas A, Del-Toro N, Dianes JA, Griss J, Lavidas I, Mayer G, Perez-Riverol Y, Reisinger F, Ternent T, Xu QW, Wang R, Hermjakob H, Nucleic Acids Res 2016, 44.

Author Manuscript Author Manuscript Author Manuscript Author Manuscript

Significance

Although the complexities of co-culture systems and the difficulty of preserving *ex vivo* retinal tissue in culture environments complicate identifying mechanisms of action, the significance of this study lies in the use of a clinically relevant cell therapeutic and animal model of retinal degeneration. From this retinal explant and hNPC co-culture assay, a number of conclusions can be drawn. First, hNPCs secrete pro survival proteins, as detected by mass spectrometry and bioinformatic analyses. Second, retinal explants have better cell survival when co-cultured with hNPCs than when cultured alone, as shown by proteomic analysis and TUNEL assay. Lastly, pathway analysis identified NRF2-mediated oxidative response signaling in both the *ex vivo* and *in vivo* settings, indicating that this may be an important mechanism that enables hNPC-induced survival. NRF2 could be potentially used as an adjuvant therapy to stem cell treatment for retinal degeneration.

Author Manuscript Author Manuscript Author Manuscript Author Manuscript

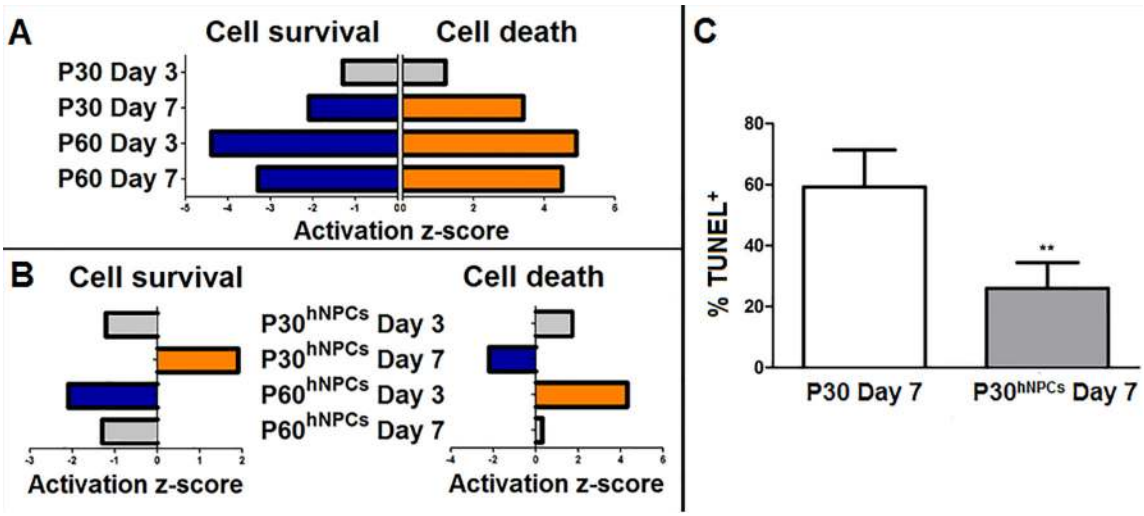

Figure 1: Proteomic analysis of in vitro retinas.

Cellular function analysis of RCS retinas cultured alone for 3 and 7 days was performed (A). Cell survival was significantly inhibited (blue bars) in P30 retina at day 7 and in P60 retinas at both days 3 and 7, whereas cell death was activated (orange bars) in the retinas at these time points. No significant activation z-score was detected in P30 retinas at 3 days in culture for either cell survival or cell death (grey bars), suggesting that there is no difference in these processes at this age and time point. P30 and P60 retinas were co-cultured with hNPCs ($P30^{hNPCs}$ and $P60^{hNPCs}$, respectively) for 3 or 7 days, and functional analysis was performed (B). Only $P30^{hNPCs}$ at Day 7 had activation of cell survival and inhibition of cell death, suggesting that hNPCs aid in retinal survival in P30 retinas by 7 days in culture. TUNEL apoptotic analysis was performed on RCS age P30 retina (C). P30 retina cultured alone had a high percentage of $TUNEL^+$ cells; however, P30 retina co-cultured with hNPCs ($P30^{hNPCs}$) had a significant decrease in the percentage of apoptotic cells (Two-tailed *t*-test, ** $p<0.05$). These results suggest that hNPCs are able to aid in retinal survival in P30 retina at 7 days in culture. At 7 days, proteins from the P30 retinas co-cultured with hNPCs were compared to P30 retinas cultured alone, and the protein profiles and fold changes were input into Ingenuity Pathway Analysis (IPA) software (Qiagen). Canonical pathway analysis detected 8 pathways (D). These pathways had significant activation z-score ≥ 2 or ≤ -2 (bars) and a -log (Benjamini-Hochberg) $p \geq 1.3$ (line). In addition, upstream analysis identified 16 predicted activated (orange) and 7 predicted inhibited (blue) upstream regulators (E).

Author Manuscript Author Manuscript Author Manuscript Author Manuscript

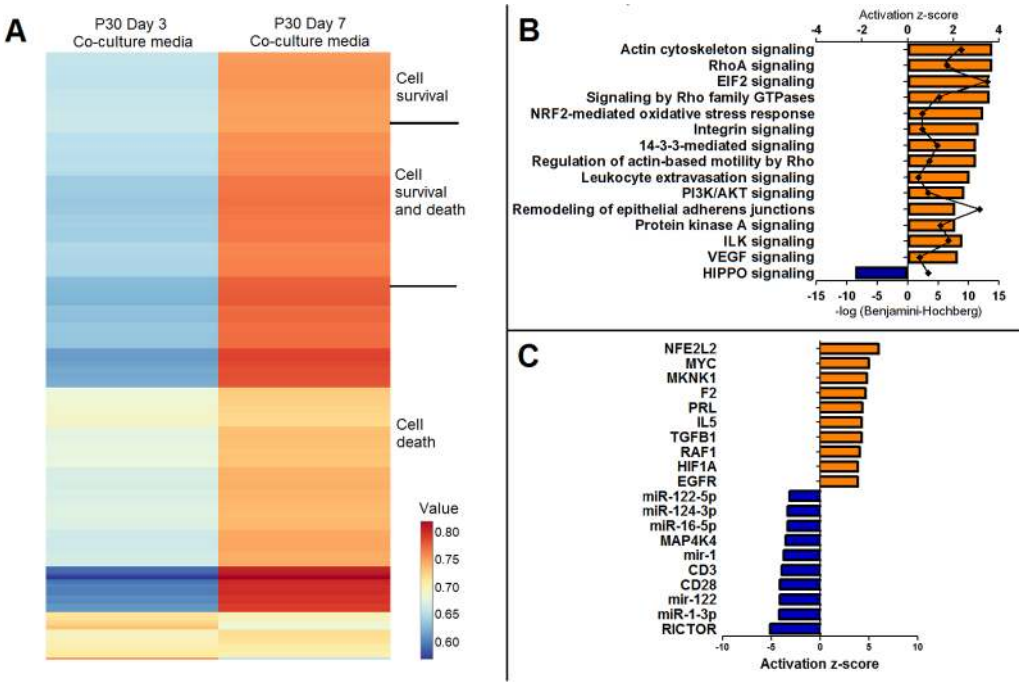

Figure 2: Proteomic analysis of hNPC-secreted factors.

Media from hNPCs co-cultured with P30 retinas were prepared for mass spectrometry, and the protein profiles were input into Ingenuity Pathway Analysis (IPA) software (Qiagen Fall 2016 Release). Cell survival was predicted to be activated (*p*-value 1.19E-14, activation z-score 3.087) and cell death was predicted to be significantly inhibited (*p*-value 1.23E-40, activation z-score −2.744) in co-cultured media from day 7. Proteins involved in the cell survival, cell death, or both signaling mechanisms have differential expression in day 7 co-cultured media (A; Supplemental Table 4). Canonical pathway analysis identified 15 signaling pathways that were affected in the co-cultured media (B). A majority of the pathways were shown to be activated (orange bars) with one inhibited (blue bar). Significance taken at –log (Benjamini-Hochberg) $p \geq 1.3$ (line graph) and activation z-score ≥ 2 or ≤ -2 (bar graph). Upstream analysis identified 143 regulators (Supplemental Table 5) with the top 10 activated (orange bars) and 10 inhibited (blue bars) regulators shown (C). Significance taken at $p < 0.05$ and activation z-score ≥ 2 or ≤ -2 (bar graph).

Author Manuscript Author Manuscript Author Manuscript Author Manuscript

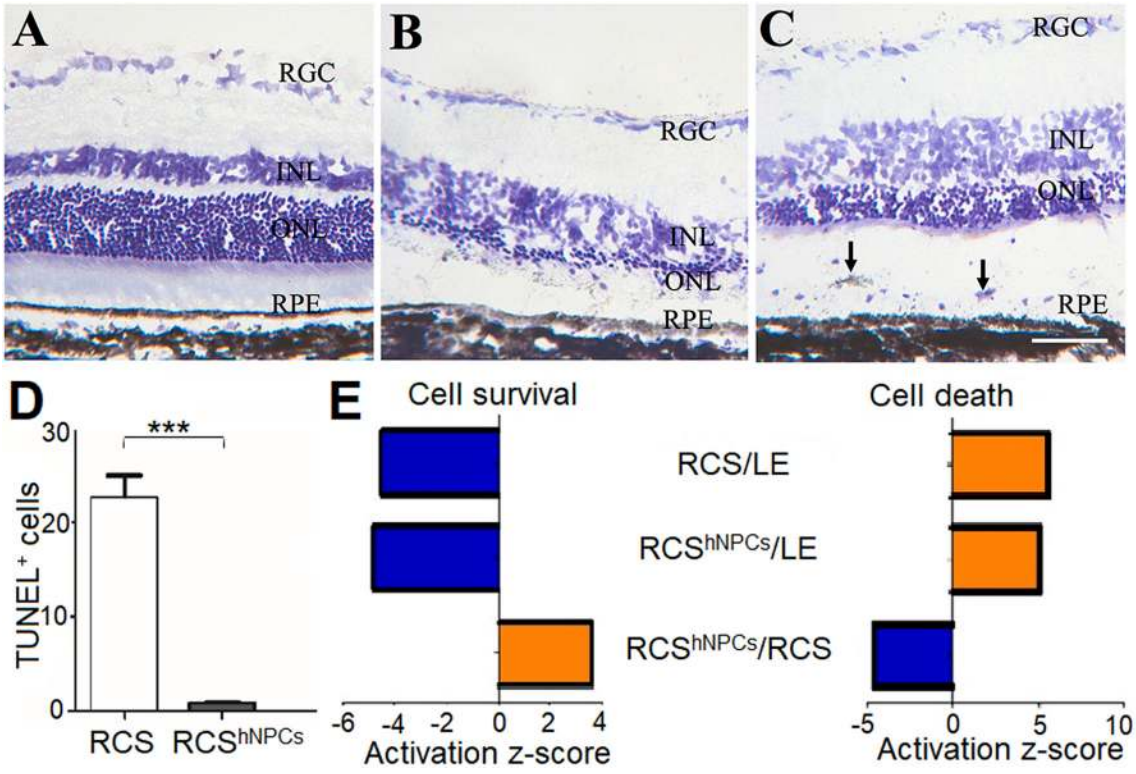

Figure 3: Retinal cell survival following hNPC injection.

By histological staining, postnatal day 60 (P60) wild-type Long Evans (LE) rats have approximately 10 layers of photoreceptor cells in the retinal outer nuclear layer (ONL; A). In age-matched untreated retinal degenerate RCS, loss of photoreceptor cells leads to only 2 to 3 layers of photoreceptors (B). RCS treated with hNPCS (RCS^{hNPCs}) have 5 to 6 layers of photoreceptor cells in areas adjacent to hNPCs (arrows; C), indicating that there is hNPC-induced photoreceptor survival. Retinal ganglion cell, RGC; inner nuclear layer, INL; outer nuclear layer, ONL; retinal pigment epithelium, RPE. Scale bar = 50 μm. TUNEL assay was performed on retina sections (D). RCS retina had a significantly higher number of $TUNEL^+$ cells than RCS retina treated with hNPCs (***, $p<0.01$), further suggesting that hNPCs play a role in photoreceptor survival. Protein profiles of LE, RCS, and RCS^{hNPCs} were compared and input into Ingenuity Pathway Analysis (IPA) software (Qiagen), and functional analysis was performed (E). Cell survival is inhibited in the RCS samples vs. LE, whereas cell survival is activated in RCS^{hNPCs} as compared to RCS (E, left). Conversely, cell death is activated in the RCS samples vs. LE, but is inhibited in RCS^{hNPCs} as compared to RCS (E, right). These results indicate that RCS^{hNPCs} have an increase in cell survival and decrease in cell death signaling. Bars shown have a –log Benjamini-Hochberg $p \geq 1.3$ and an activation z-score ≥ 2 or ≤ -2, orange bars indicate activation and blue bars indicate inhibition.

Author Manuscript Author Manuscript Author Manuscript Author Manuscript

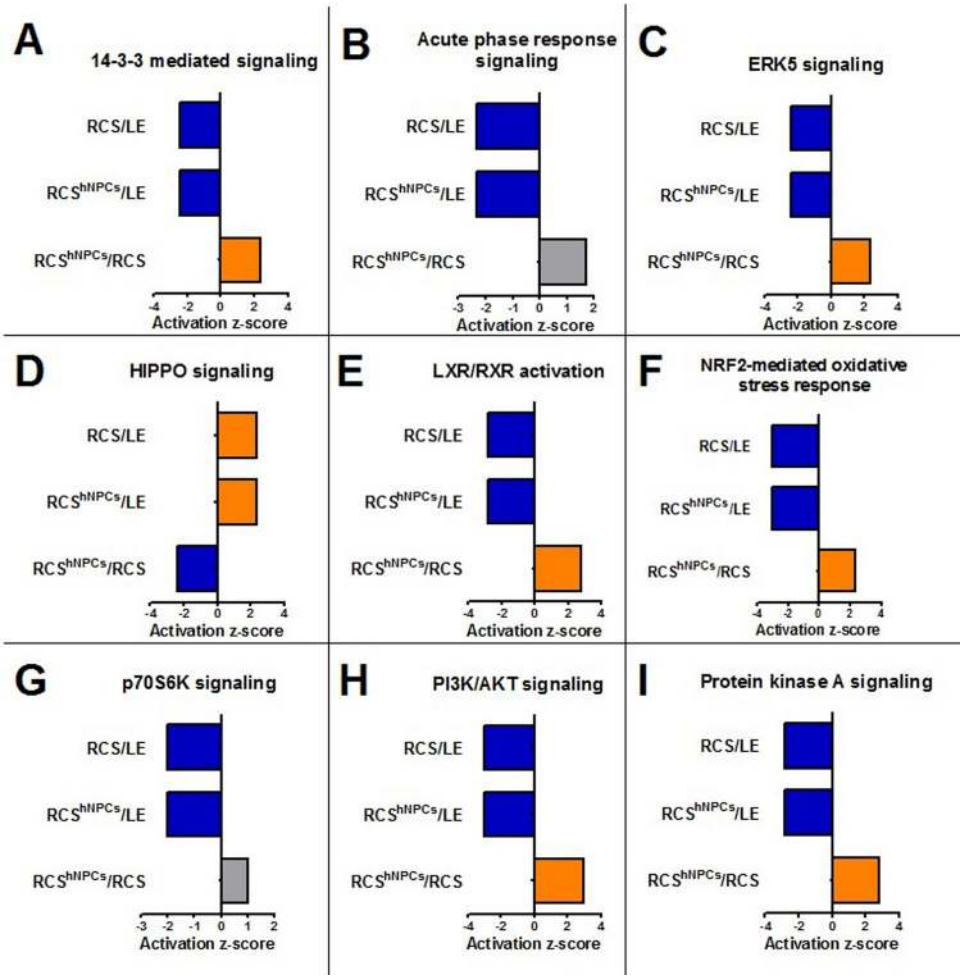

Figure 4: Canonical pathways identified in comparisons of in vivo retinal tissue.

LE, RCS, and RCS^{hNPCs} protein profiles were compared and 9 pathways were found to be significantly different between the samples (-log Benjamini-Hochberg p ≥1.3 and activation z-score ≥2 or ≤−2). Six pathways were inhibited in RCS samples as compared to wild-type Long Evans (LE), but were significantly activated in RCS^{hNPCs}/RCS (A, C, E, F, H, and I). Similarly, one pathway was activated in RCs samples as compared to LE and was significantly inhibited in RCS^{hNPCs}/RCS (D), suggesting protein and signaling changes occur with hNPC treatment. Two pathways were inhibited in RCS compared to LE but had no significant activation z-score in RCS^{hNPCs}/RCS (B and G). Blue bars denote inhibition with significant z-score ≤−2, orange bars indicate activation with significant z-score ≥2, grey bars symbolize non-significant z-score for either inhibition or activation.

Author Manuscript Author Manuscript Author Manuscript Author Manuscript

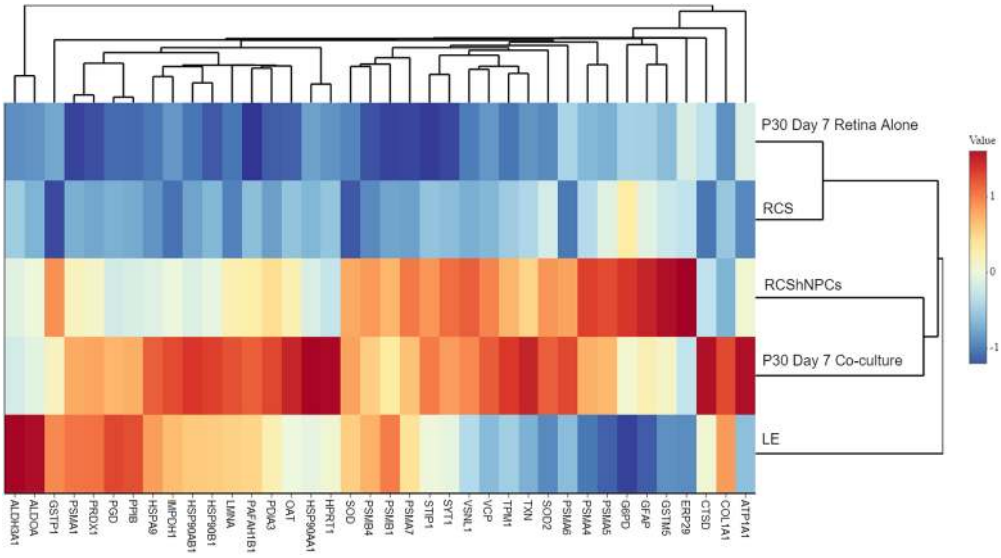

Figure 5: In vitro and in vivo hierarchical cluster analysis of NRF2-mediated oxidative stress response signaling.

The NRF2-mediated oxidative stress response was a significantly upregulated pathway in both the *in vitro* and *in* vivo protein comparisons. Downstream proteins regulated by NRF2 were identified and compared between the *in vitro* and *in vivo* data sets. P30 retinas cultured alone and untreated RCS retinas display similar downregulation of key NRF2 proteins. P30 retinas co-cultured with hNPCs and RCS^{hNPCs} upregulate NRF2-mediated oxidative stress response signaling proteins, suggesting hNPCs induce protein expression changes more similar to wild-type LE retinas. Value is the distance from the mean of the $\log_2$ expression level.

Author Manuscript Author Manuscript Author Manuscript Author Manuscript

Table 1:
Samples processed for proteomic analysis.

Ex vivo retinas were cultured from P30 and P60 RCS rats with hNPCs ($P30^{hNPCs}$/$P60^{hNPCs}$) or alone for 3 or 7 days. Retinas and media were collected from these *ex vivo* experiments for preparation for mass spectrometry. Additionally, retinas from wild-type LE, retinal degenerate RCS, and RCS treated with hNPCs (RCS^{hNPCs}) rats collected and prepared for proteomic analysis (n=3 for each sample type).

Sample Name	Sample Type	Age of Retina	Experiment Type	Days in Culture	hNPCs?
P30 Day 3 Retina	Retina	P30	Ex vivo	3	N
P30 Day 7 Retina	Retina	P30	Ex vivo	7	N
P60 Day 3 Retina	Retina	P60	Ex vivo	3	N
P60 Day 7 Retina	Retina	P60	Ex vivo	7	N
$P30^{hNPCs}$ Day 3 Retina	Retina	P30	Ex vivo	3	Y
$P30^{hNPCs}$ Day 7 Retina	Retina	P30	Ex vivo	7	Y
$P60^{hNPCs}$ Day 3 Retina	Retina	P60	Ex vivo	3	Y
$P60^{hNPCs}$ Day 7 Retina	Retina	P60	Ex vivo	7	Y
P30 Day 3 Retina	Media	P30	Ex vivo	3	N
P30 Day 7 Retina	Media	P30	Ex vivo	7	N
$P30^{hNPCs}$ Day 3 Co-culture	Media	P30	Ex vivo	3	Y
$P30^{hNPCs}$ Day 7 Co-culture	Media	P30	Ex vivo	7	Y
LE - 1	Retina	P60	In vivo	n/a	N
LE - 2	Retina	P60	In vivo	n/a	N
LE - 3	Retina	P60	In vivo	n/a	N
RCS - 1	Retina	P60	In vivo	n/a	N
RCS - 2	Retina	P60	In vivo	n/a	N
RCS - 3	Retina	P60	In vivo	n/a	N
RCS^{hNPCs} - 1	Retina	P60	In vivo	n/a	N
RCS^{hNPCs} - 2	Retina	P60	In vivo	n/a	N
RCS^{hNPCs} - 3	Retina	P60	In vivo	n/a	N